

Comparison of the Effects on Stator Currents Between Continuous Model and Discrete Model of the Three-phase Induction Motor in the Presence of Electrical Parameter Variations

1st Larizza Delorme 


Master Student in Electronic Engineering
Universidad del Cono Sur de las Américas (UCSA)
Asuncion, Paraguay
laridelorme@gmail.com

3th Jorge Rodas 

Laboratory of Power and Control Systems (LSPyC)
Universidad Nacional de Asunción
Luque, Paraguay
jrodas@ing.una.py

5th Osvaldo Gonzalez 


Laboratory of Power and Control Systems (LSPyC)
Universidad Nacional de Asunción
Luque, Paraguay
ogonzalez@ing.una.py

2nd Magno Ayala 

Laboratory of Power and Control Systems (LSPyC)
Universidad Nacional de Asunción
Luque, Paraguay
mayala@ing.una.py

4th Raul Gregor 

Laboratory of Power and Control Systems (LSPyC)
Universidad Nacional de Asunción
Luque, Paraguay
rgregor@ing.una.py

6th Jesus Doval-Gandoy 

Applied Power Electronics Technology Research Group (APET)
Universidad de Vigo
Vigo, Spain
jdoval@uvigo.es

Abstract—Three-phase induction motors are the most widely used electrical energy conversion machines due to their low cost, robustness, and ease of maintenance. Hence, the mathematical model analysis is fundamental to comprehend the behavior of the machine in order to implement a certain type of control. This article presents a comparison between the effects on the current, in steady-state, of electrical parameter variations of a three-phase induction motor model based on discrete-time with a continuous model by considering electrical parameters fixed in nominal values. Side by side comparisons between the application of pure sinusoidal waveforms and PWM waveforms generated by a voltage source inverter to the induction motor are presented. Simulation results are provided to show the parameter with the most significant impact over the machine when varying values.

Index Terms—Induction motors, magnetization inductance, predictive discretized model.

I. INTRODUCTION

Historically, one of the most used drives in industrial applications have been the induction machines due to some specific characteristics such as low cost, robustness and ease of maintenance [1]. As a consequence, the interest in the use of induction motor (IM) drives has allowed the development of well-established control techniques as field oriented control, direct torque control and, more recently, model predictive control (MPC) [2]–[5]. However, to apply control techniques, it is important to have a finished model to describe the

properties of the physical system precisely in order to be controlled optimally [6]. In the design of the mathematical model of IMs, it is necessary to know the electrical and mechanical parameters. Some of these can be provided by the manufacturer or can be obtained through standardized tests [7], but in operation, these values, which are assumed as nominal in the equivalent circuit, vary according to different load conditions and effects such as temperature, magnetic saturation, skin effect, harmonics and rotor movement [1], [7], [8].

A precise knowledge of the parameter values is essential to determine a suitable model. When vector control or non-linear control techniques are used [9]–[11], such as the MPC, the control efficiency depends on the model to predict the states and to produce the desired performance [12]. For instance, in accurate speed estimation for the operation of speed-sensorless using machine model-based approaches [13]–[15]. In previous works, parameter identification processes are presented to obtain values focused on the magnetization inductance as in [1], [16]–[18] or focused on rotor and stator resistances as in [16], [19]. In other works, mathematical models are proposed considering magnetic saturation as in [20], [21].

Generally, parameters like stator and rotor resistance as well as magnetization inductance are considered constant in the model for simplicity without knowing how much this affects

the performance of the electric drive. This paper aims to present a quantitative analysis of the impact on the currents of the electrical parameter variations in the discrete model concerning the continuous model with nominal values of the IM, in terms of the Mean Square Error (MSE). Variations are applied by taking into account several values in a range and comparisons of the effect between an operation of the IM with pure sinusoidal waveforms and voltage source inverter are presented.

The rest of this paper is organized as follows. The IM mathematical model in continuous time is presented in Section II. Then, in Section III, the model of the IM in discrete-time is described. In order to compare the effects of the variations, two types of power supply are exposed in Section IV. In Section V, simulation tests are described, and the results of the parameter variations is examined. Finally, conclusions are presented in the last section.

II. IM MATHEMATICAL MODEL

The dynamic model of the three-phase IM can be expressed in the stationary reference frame α - β such as:

$$\begin{aligned} \mathbf{v}_s &= R_s \mathbf{i}_s + \frac{d\boldsymbol{\lambda}_s}{dt} \\ 0 &= R_r \mathbf{i}_r + \frac{d\boldsymbol{\lambda}_r}{dt} - j\omega_r \boldsymbol{\lambda}_r \\ \boldsymbol{\lambda}_s &= L_s \mathbf{i}_s + L_m \mathbf{i}_r \\ \boldsymbol{\lambda}_r &= L_m \mathbf{i}_s + L_r \mathbf{i}_r \end{aligned} \quad (1)$$

where R_s and R_r are the stator and rotor resistances, respectively, L_m is the magnetizing inductance, L_s and L_r are the stator and rotor inductances, \mathbf{v}_s , \mathbf{i}_s , \mathbf{i}_r are the stator voltage vector, the stator current and the rotor current vectors, $\boldsymbol{\lambda}_s$ and $\boldsymbol{\lambda}_r$ are the stator and rotor flux vectors. All electrical variables mentioned in (1) are two-dimensional complex space vector where the real and imaginary part denotes the components in the α - β plane. A general block diagram is represented in Fig. 1.

The electromagnetic torque can be expressed by:

$$T_e = \frac{3}{2} p_p \frac{L_m}{L_r} \text{Im} \{ \bar{\boldsymbol{\lambda}}_r \mathbf{i}_s \} \quad (2)$$

where p_p is the number of pole pairs and $\bar{\boldsymbol{\lambda}}_r$ is the complex conjugate of the rotor flux vector. In order to describe the behavior of the mechanical speed ω_m and the electric rotor speed ω_r according to the electromagnetic torque T_e and load torque T_l , the mechanical equation is given by:

$$J \frac{d\omega_m}{dt} + B \omega_m = T_e - T_l \quad (3)$$

where J is the inertia of the mechanical shaft and B the friction coefficient. The mechanical speed in terms of electrical rotor speed is defined as:

$$\omega_m = \frac{\omega_r}{p_p}. \quad (4)$$

The continuous model (1)-(4) can be represented using the state-space representation as follows:

$$\begin{aligned} \dot{\mathbf{x}}(t) &= \mathbf{A}\mathbf{x}(t) + \mathbf{B}\mathbf{u}(t) \\ \mathbf{y}(t) &= \mathbf{C}\mathbf{x}(t) \end{aligned} \quad (5)$$

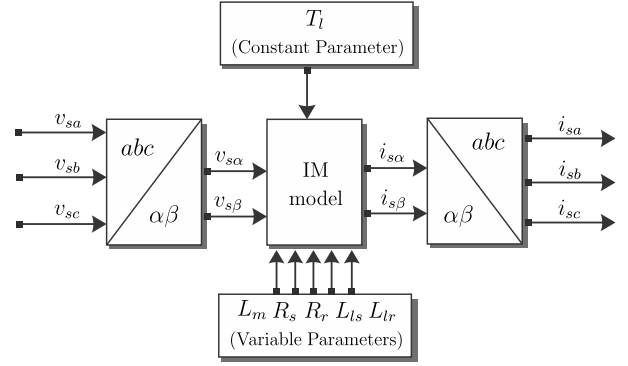


Fig. 1. Block diagram of the IM model.

where: $\mathbf{x}(t) = [i_{s\alpha}, i_{s\beta}, \lambda_{r\alpha}, \lambda_{r\beta}]^T$ represent the state vector considering the stator current and the rotor flux variables, $\mathbf{u}(t) = [v_{s\alpha}, v_{s\beta}]^T$ are the voltage input applied to the stator, and $\mathbf{y}(t)$ denotes the output vector. The superscript (T) is used to denote the transposed matrix and to define the dynamic of the electrical drive are used the matrices \mathbf{A} , \mathbf{B} and \mathbf{C} . Then:

$$\mathbf{A} = \begin{bmatrix} c_1 & 0 & c_2 & c_3\omega_r \\ 0 & c_1 & -c_3\omega_r & c_2 \\ c_5 & 0 & c_6 & -\omega_r \\ 0 & c_5 & \omega_r & c_6 \end{bmatrix} \quad (6)$$

$$\mathbf{B} = \begin{bmatrix} c_4 & 0 \\ 0 & c_4 \\ 0 & 0 \\ 0 & 0 \end{bmatrix} \quad (7)$$

$$\mathbf{C} = \begin{bmatrix} 1 & 0 & 0 & 0 \\ 0 & 1 & 0 & 0 \\ 0 & 0 & 0 & 0 \\ 0 & 0 & 0 & 0 \end{bmatrix} \quad (8)$$

where:

$$\begin{aligned} c_1 &= -\left(\frac{R_s}{\sigma L_s} + \frac{L_m^2}{\sigma L_s L_r \tau_r}\right) & c_2 &= \frac{L_m}{\sigma L_s L_r \tau_r} & c_3 &= \frac{L_m}{\sigma L_s L_r} \\ c_4 &= \frac{1}{\sigma L_s} & c_5 &= \frac{L_m}{\tau_r} & c_6 &= -\frac{1}{\tau_r} \\ \sigma &= 1 - \frac{L_m^2}{L_s L_r} & \tau_r &= \frac{L_r}{R_r}. \end{aligned}$$

III. DISCRETE-TIME IM MODEL

The first order Euler approximation is applied in order to predict the state variables in the next sampling time and to keep computing cost low. The derived approximation is given by:

$$\dot{\mathbf{x}} \simeq \frac{\mathbf{x}(k+1) - \mathbf{x}(k)}{T_s} \quad (9)$$

where x is the state variable, T_s is the sampling time and k represent the current sample.

Using (9) and (5), can be rewritten as:

$$\mathbf{x}(k+1) = (\mathbf{I} + \mathbf{A}T_s)\mathbf{x}(k) + \mathbf{B}T_s\mathbf{u}(k) \quad (10)$$

where $\mathbf{x}(k) = [i_{s\alpha}(k), i_{s\beta}(k), \lambda_{r\alpha}(k), \lambda_{r\beta}(k)]^T$, \mathbf{I} is the identity matrix and $\mathbf{u}(k) = [v_{s\alpha}(k), v_{s\beta}(k)]^T$.

IV. TYPES OF THREE-PHASE INDUCTION MOTOR POWER SUPPLIES

In this section, two types of three-phase IM power supplies are described. These are considered in the analysis of impact of parameter variations.

A. Pure Sinusoidal Waveforms

This method consists of the direct connection of the stator windings to three-phase voltages sinusoidal, which have a 120 degree phase shift between each other, with the amplitude and frequency adjusted to the IM nominal voltage values.

B. Three-phase voltage source inverter

One of the most used configurations of power electronic converters consists of an uncontrolled rectifier connected to a voltage source inverter (VSI) through a DC-Link. Fig. 2 shows the three-phase inverter which has three legs, each consisting of two electronic switches. The output of the VSI corresponds to each midpoint between these switches. A three-phase VSI with pulse width modulation (PWM) allows the control of the three-phase output voltages in amplitude and frequency through three sinusoidal reference voltages of controlled amplitude. In the PWM technique, each reference voltage is compared to a triangular waveform, the comparator's output defines the switching states used to drive the inverter switches.

The triangular waveform has a switching frequency that sets the frequency at which the switches will operate. On the other hand, the sinusoidal reference signal has the desired fundamental frequency of the inverter voltage output.

The output voltages of the inverter v_{zN} with respect to the negative bus of the DC-link N , are defined by the switching states S_z in each leg as follow:

$$v_{zN} = V_{dc}S_z \quad (11)$$

where the phases are represented by $z = [a, b, c]$.

Considering balanced operating conditions, the relationship between the phase voltages of the VSI output v_{zN} with the phase voltages v_{zn} and the negative DC-link bus voltages v_{nN} is expressed by:

$$\begin{aligned} v_{zn} &= v_{zN} - v_{nN} \\ &= V_{dc}S_z - \frac{1}{3}(v_{aN} + v_{bN} + v_{cN}) \end{aligned} \quad (12)$$

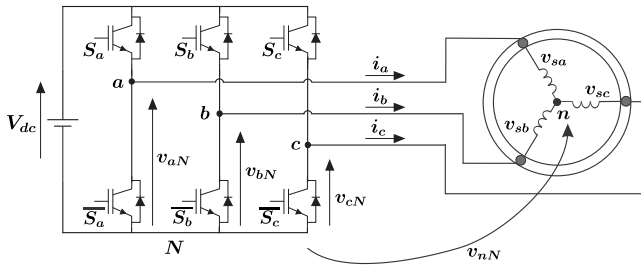


Fig. 2. VSI scheme connected to a 3-phase IM.

TABLE I
MECHANICAL AND ELECTRICAL PARAMETERS OF IM

Parameter	Value	Parameter	Value
R_s	0.7384 Ω	p_p	2
R_r	0.7402 Ω	B	0.000503 kg.m ² /s
L_{ls}^*	3.045 mH	J	0.0343 kg.m ²
L_{lr}^*	3.045 mH	Nominal speed	1440 rpm
L_s	127.1 mH	Nominal power	7.5 kW
L_r	127.1 mH	Voltage (line-line)	400 V
L_m	124.1 mH	Nominal frequency	50 Hz

*Are the leakage inductances. $L_s = L_{ls} + L_m$ and $L_r = L_{lr} + L_m$

where v_{zn} are the voltages on IM stator windings with star connection, v_{sa} , v_{sb} and v_{sc} .

The output voltages provided by the VSI are not purely sinusoidal, since it provides discrete output voltages which contain components of higher frequencies multiples of the fundamental frequency [22], [23].

V. ANALYSIS METHOD AND SIMULATIONS

The simulations of the three-phase IM in open loop, for both mentioned models, are implemented using MATLAB/Simulink software. Table I presents the mechanical and electrical parameters of the IM under study. In all cases, constant load conditions of 25% of the nominal value is applied. Sampling time of 10 μ s is considered.

Initially, a balanced set of three-phase, fundamental harmonic voltages, adjusted at the nominal voltage of the machine, are applied to the IM continuous model and the output currents in steady-state are obtained, disregarding the magnetic saturation effect, and by considering L_m , R_s , R_r , L_{ls} , and L_{lr} , constant in their nominal values.

The same power supply is applied to the discrete model and a single parameter is varied, measured and compared at once. The variation of the electrical parameters values are realized taking 13 points in a range of $\pm 30\%$ of their nominal values. Obtained results for the stator currents $i_{s\alpha}$ in steady-state applied to the IM discrete model, are shown in Fig. 3 and Fig. 4.

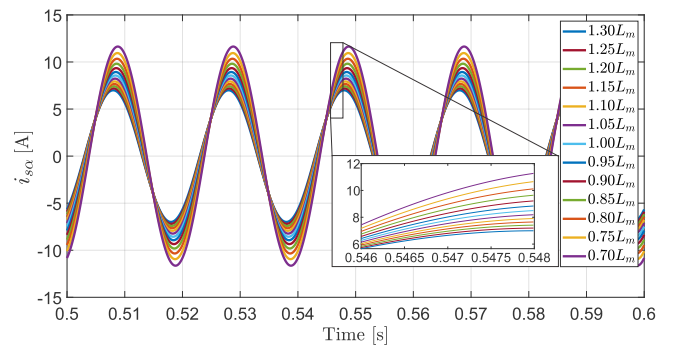


Fig. 3. Results of the current $i_{s\alpha}$ in steady-state, varying L_m parameter value and by applying three-phase sinusoidal waveforms at the IM discrete model.

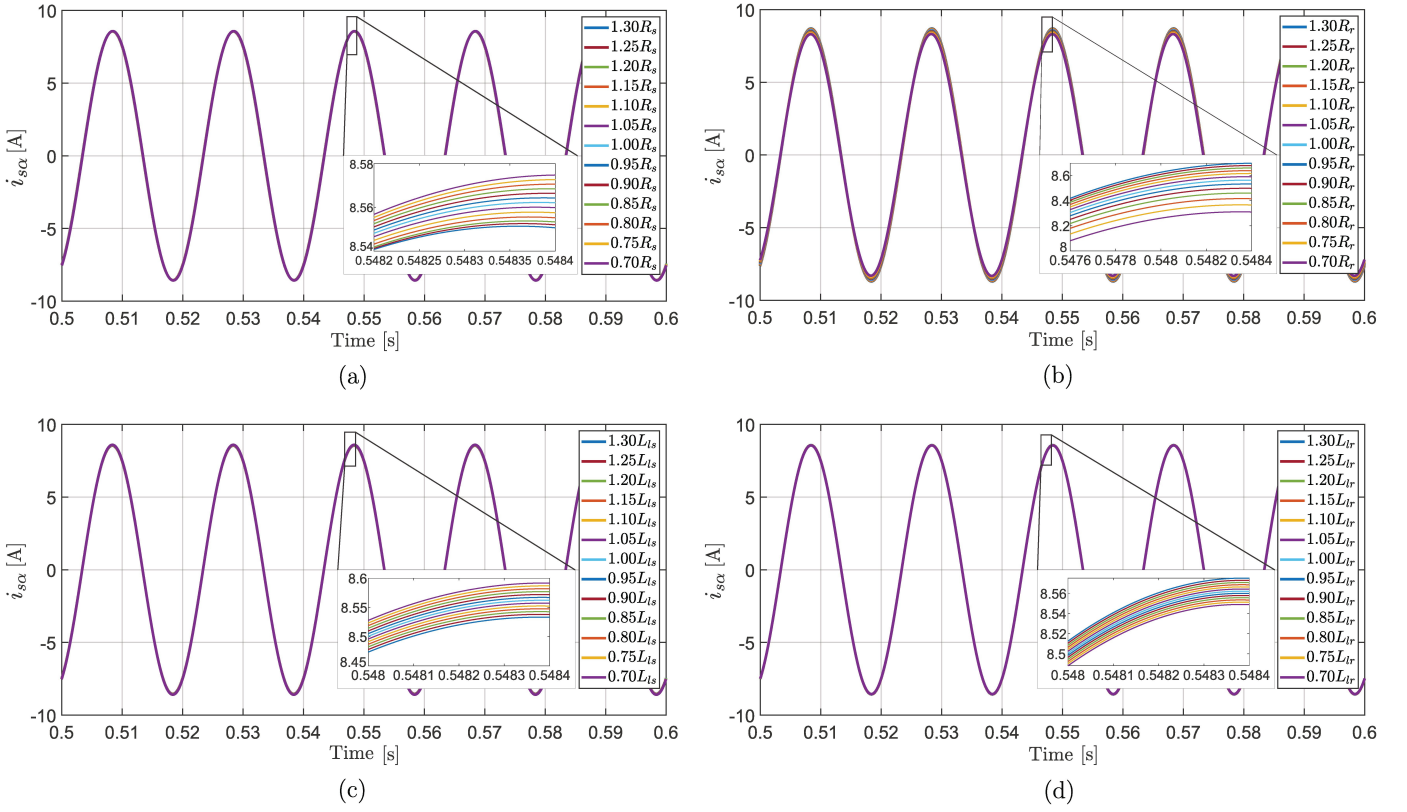


Fig. 4. Results of the current $i_{s\alpha}$ in steady-state, varying the parameter values: (a) R_s ; (b) R_r ; (c) L_{ls} ; (d) L_{lr} , and by applying three-phase sinusoidal waveforms at the IM discrete model.

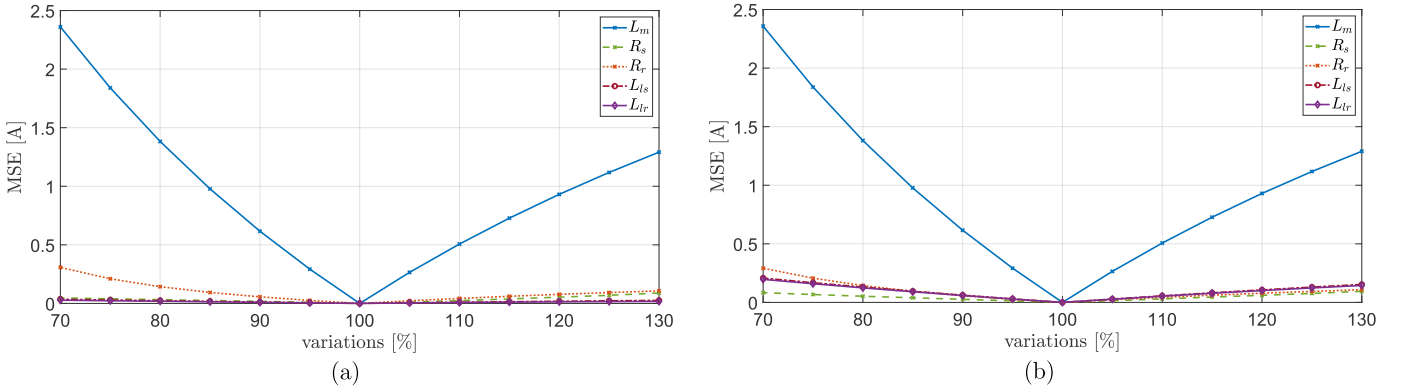


Fig. 5. MSE by considering the parameters variations in an IM model: (a) applying pure sinusoidal waveforms; (b) applying three-phase VSI.

The quantitative indicator, used to represent differences between the discrete model and the continuous model, is obtained by analyzing the results of the currents in steady-state of both models and by calculating the MSE between the stator currents obtained in continuous model $i_s^*(k)$ with electrical parameters fixed at the nominal values and the stator currents obtained in discrete model $i_s(k)$ considering the range of parameter variations above mentioned. MSE is given by:

$$\text{MSE} = \sqrt{\frac{1}{n} \sum_{k=m+1}^{m+n} (i_s^*(k) - i_s(k))^2} \quad (13)$$

where n is the total number of samples taken in an interval, and m is the number taken as a starting point in steady-state. Both are represented by integer numbers.

By calculating the MSE for the stator currents $i_{s\alpha}$ and comparing, taking into account 13 variation points of each parameter, the results can be seen in Fig. 5(a). The curve that corresponds to the variation of the magnetization inductance represents the variable with the most significant impact on the MSE of the stator currents between the discrete model and continuous model, being L_m present in practically all the equations of the three-phase IM mathematical model. Table II

TABLE II
STEADY STATE ANALYSIS OF MSE OF THE STATOR CURRENTS IN α - β PLANE AT DIFFERENT VALUES OF THE ELECTRICAL PARAMETERS BY APPLYING THREE PURE SINUSOIDAL VOLTAGE

%	L_m [H]	MSE [A]	R_s [Ω]	MSE [A]	R_r [Ω]	MSE [A]	L_{ls} [H]	MSE [A]	L_{lr} [H]	MSE [A]
70	0.0869	2.3600	0.5169	0.0470	0.5181	0.3075	0.0021	0.0355	0.0021	0.0277
75	0.0931	1.8398	0.5538	0.0397	0.5552	0.2103	0.0023	0.0291	0.0023	0.0228
80	0.0993	1.3826	0.5907	0.0323	0.5922	0.1428	0.0024	0.0233	0.0024	0.0184
85	0.1055	0.9777	0.6276	0.0250	0.6292	0.0938	0.0026	0.0176	0.0026	0.0140
90	0.1117	0.6166	0.6646	0.0176	0.6662	0.0562	0.0027	0.0116	0.0027	0.0094
95	0.1179	0.2925	0.7015	0.0094	0.7032	0.0258	0.0029	0.0057	0.0029	0.0046
100	0.1241	0.0000	0.7384	0.0000	0.7402	0.0000	0.0030	0.0000	0.0030	0.0000
105	0.1303	0.2653	0.7753	0.0112	0.7772	0.0226	0.0032	0.0053	0.0032	0.0043
110	0.1365	0.5069	0.8122	0.0243	0.8142	0.0428	0.0033	0.0102	0.0033	0.0080
115	0.1427	0.7281	0.8492	0.0384	0.8512	0.0610	0.0035	0.0146	0.0035	0.0110
120	0.1489	0.9311	0.8861	0.0532	0.8882	0.0777	0.0037	0.0187	0.0037	0.0135
125	0.1551	1.1182	0.9230	0.0693	0.9253	0.0930	0.0038	0.0224	0.0038	0.0155
130	0.1631	1.2913	0.9599	0.0890	0.9623	0.1072	0.0040	0.0260	0.0040	0.0171

TABLE III
COMPARATIVE OF MSE OF THE STATOR CURRENTS IN α - β PLANE BY APPLYING THREE PURE SINUSOIDAL VOLTAGE RESPECT TO MSE USING THREE-PHASE VSI ON THE IM AT DIFFERENT VALUES OF THE L_m AND R_r

%	L_m [H]	MSE [A]	VSI-MSE [A]	R_r [Ω]	MSE [A]	VSI-MSE [A]
70	0.0869	2.3600	2.3578	0.5181	0.3075	0.2915
75	0.0931	1.8398	1.8381	0.5552	0.2103	0.2070
80	0.0993	1.3826	1.3814	0.5922	0.1428	0.1436
85	0.1055	0.9777	0.9768	0.6292	0.0938	0.0950
90	0.1117	0.6166	0.6160	0.6662	0.0562	0.0570
95	0.1179	0.2925	0.2922	0.7032	0.0258	0.0261
100	0.1241	0.0000	0.0000	0.7402	0.0000	0.0000
105	0.1303	0.2653	0.2650	0.7772	0.0226	0.0228
110	0.1365	0.5069	0.5065	0.8142	0.0428	0.0431
115	0.1427	0.7281	0.7274	0.8512	0.0610	0.0615
120	0.1489	0.9311	0.9303	0.8882	0.0777	0.0784
125	0.1551	1.1182	1.1172	0.9253	0.0930	0.0939
130	0.1631	1.2913	1.2901	0.9623	0.1072	0.1083

exposes the values of the MSE for each parameter variation under study. As can be seen, L_m reaches the highest MSE in magnetic saturation condition (low L_m). The next parameter that has a significant effect is R_r which shows a higher effect on stator currents MSE at low values. Still the MSE effect is approximately of 13% of L_m effect. The other parameters show an impact of approximately between 1% to 2% of L_m effect, being considered insignificant compared to L_m and R_r variations.

The same procedures described for evaluating the effect of parameter variations by applying three-phase pure sinusoidal voltage are performed using the three-phase VSI with carrier-based sinusoidal PWM, on both models. In Fig. 5(b), it can be noticed the magnetization inductance continues to have a greater impact than the other parameters on the stator current error. However, the impact of the rotor resistance represents approximately 12.3%, stator resistance 3.5% and the leakage

inductances about 8.8%, at low values, with respect to the L_m effect.

Table III shows the comparison between the two types of IM power supplies in terms of the MSE of the stator current in steady-state and the variations of the L_m and R_r values.

VI. CONCLUSION

In this paper, a discrete model of an IM with electrical parameter variations is compared with a continuous model where the electrical parameters are fixed in nominal values. In order to determine the effects on the stator current in a steady-state, the variations of the parameters are made in a range of 70% to 130% of nominal values and the errors are represented in terms of the MSE. The results of the analysis of the MSE of stator currents, in steady-state, with the variations of the parameters such as magnetization inductance, stator resistance, rotor resistance, leakage inductance of the stator and rotor, show that variations of the leakage inductances and

stator resistance have an insignificant impact on the current. However, the variation of the rotor resistance is more notorious and the magnetization inductance has a the greatest impact in the IM powered by three-phase sinusoidal sources and with a three-phase VSI. Taking these conclusions into account, an analysis of the effects of variations of the electrical parameters on a closed-loop system by implementing a model-based control will be presented in future work.

ACKNOWLEDGMENT

The authors would like to thank the financial support from the Paraguayan Science and Technology National Council (CONACYT) through Grant Number POSG17-69.

REFERENCES

- [1] M. Matsushita, F. Ishibashi, and S. Mizuno, "Calculation of magnetizing inductance and magnetizing current of squirrel cage induction motor," in *19th International Conference on Electrical Machines and Systems (ICEMS)*, November 2016, pp. 1–5.
- [2] F. Wang, S. Li, X. Mei, W. Xie, J. Rodriguez, and R. M. Kennel, "Model-based predictive direct control strategies for electrical drives: An experimental evaluation of PTC and PCC methods," *IEEE Transactions on Industrial Informatics*, vol. 11, no. 3, pp. 671–681, June 2015.
- [3] A. Favato, P. G. Carlet, F. Toso, and S. Bolognani, "A novel formulation of continuous control set mpc for induction motor drives," in *IEEE International Electric Machines Drives Conference (IEMDC)*, May 2019, pp. 2196–2202.
- [4] M. Ayala, J. Doval-Gandoy, J. Rodas, O. Gonzalez, and R. Gregor, "Current control designed with model based predictive control for six-phase motor drives," *ISA Transactions*, 2019.
- [5] O. Gonzalez, M. Ayala, J. Rodas, R. Gregor, G. Rivas, and J. Doval-Gandoy, "Variable-speed control of a six-phase induction machine using predictive-fixed switching frequency current control techniques," in *9th IEEE International Symposium on Power Electronics for Distributed Generation Systems (PEDG)*, June 2018, pp. 1–6.
- [6] E. Levi, "Impact of iron loss on behavior of vector controlled induction machines," *IEEE Transactions on Industry Applications*, vol. 31, no. 6, pp. 1287–1296, 1995.
- [7] M. Kral and R. Gono, "Dynamic model of asynchronous machine," in *18th International Scientific Conference on Electric Power Engineering (EPE)*, May 2017, pp. 1–4.
- [8] S. A. A. Maksoud and T. V. Chestyunina, "Simulation and experimental increased temperature effect on induction motor parameters," in *XIV International Scientific-Technical Conference on Actual Problems of Electronics Instrument Engineering (APEIE)*, October 2018, pp. 258–263.
- [9] Y. Kali, J. Rodas, M. Saad, J. Doval-Gandoy, and R. Gregor, "Nonlinear backstepping with time delay estimation for six-phase induction machine," in *IEEE International Electric Machines Drives Conference (IEMDC)*, May 2019, pp. 1798–1804.
- [10] Y. Kali, M. Saad, J. Doval-Gandoy, J. Rodas, and K. Benjelloun, "Discrete sliding mode control based on exponential reaching law and time delay estimation for an asymmetrical six-phase induction machine drive," *IET Electric Power Applications*, vol. 13, no. 11, pp. 1660–1671, 2019.
- [11] Y. Kali, J. Rodas, M. Saad, R. Gregor, K. Benjelloun, J. Doval-Gandoy, and G. Goodwin, "Speed control of a five-phase induction motor drive using modified super-twisting algorithm," in *International Symposium on Power Electronics, Electrical Drives, Automation and Motion (SPEEDAM)*, June 2018, pp. 938–943.
- [12] J. Rodriguez and P. Cortes, *Predictive control of power converters and electrical drives*. John Wiley & Sons, 2012, vol. 40.
- [13] A. Taheri and M. Mohammadbeigi, "Speed sensor-less estimation and predictive control of six-phase induction motor using extended Kalman filter," in *The 5th Annual International Power Electronics, Drive Systems and Technologies Conference (PEDSTC)*, February 2014, pp. 13–18.
- [14] M. Ayala, O. Gonzalez, J. Rodas, R. Gregor, and J. Doval-Gandoy, "A speed-sensorless predictive current control of multiphase induction machines using a Kalman filter for rotor current estimator," in *International Conference on Electrical Systems for Aircraft, Railway, Ship Propulsion and Road Vehicles International Transportation Electrification Conference (ESARS-ITEC)*, November 2016, pp. 1–6.
- [15] E. Zerdali and M. Barut, "The comparisons of optimized extended kalman filters for speed-sensorless control of induction motors," *IEEE Transactions on Industrial Electronics*, vol. 64, no. 6, pp. 4340–4351, June 2017.
- [16] H. A. Toliyat, E. Levi, and M. Raina, "A review of RFO induction motor parameter estimation techniques," *IEEE Transactions on Energy Conversion*, vol. 18, no. 2, pp. 271–283, June 2003.
- [17] M. S. Zaky, M. M. Khater, H. Yasin, and S. S. Shokralla, "Magnetizing inductance identification algorithm for operation of speed-sensorless induction motor drives in the field weakening region," in *12th International Middle-East Power System Conference (MEPCON)*, March 2008, pp. 103–108.
- [18] L. Liu, Y. Guo, and J. Wang, "Online identification of mutual inductance of induction motor without magnetizing curve," in *Annual American Control Conference (ACC)*, June 2018, pp. 3293–3297.
- [19] B. M. Chandra and S. T. Kalyani, "Online estimation of stator resistance in vector control of induction motor drive," in *IEEE Fifth India International Conference on Power Electronics (ICPE)*, December 2012, pp. 1–5.
- [20] O. Kiselychnyk, M. Bodson, and J. Wang, "Comparison of two magnetic saturation models of induction machines and experimental validation," *IEEE Transactions on Industrial Electronics*, vol. 64, no. 1, pp. 81–90, January 2017.
- [21] B. Karanayil, M. F. Rahman, and C. Grantham, "On-line rotor resistance identification for induction motor drive with artificial neural networks supported by a simple pi stator resistance estimator," in *The Fifth International Conference on Power Electronics and Drive Systems (PEDS)*, vol. 1, November 2003, pp. 433–438 Vol.1.
- [22] N. Mohan, T. M. Undeland, and W. P. Robbins, *Power electronics: converters, applications, and design*. John Wiley & Sons, 2003.
- [23] Keliang Zhou and Danwei Wang, "Relationship between space-vector modulation and three-phase carrier-based PWM: a comprehensive analysis [three-phase inverters]," *IEEE Transactions on Industrial Electronics*, vol. 49, no. 1, pp. 186–196, February 2002.